ELSEVIER

Electroencephalography and clinical Neurophysiology 96 (1995) 121–134

# Somatotopy of human hand somatosensory cortex revealed by dipole source analysis of early somatosensory evoked potentials and 3D-NMR tomography

Helmut Buchner [a,*], Ludwig Adams [b], Alice Müller [a], Irene Ludwig [a], Achim Knepper [b], Armin Thron [c], Klaus Niemann [d], Michael Scherg [e]

[a] *Department of Neurology, Klinikum RWTH, Pauwelstrasse 30, D-52057 Aachen, FRG*
[b] *Institute of Measurement Technology, RWTH, Aachen, FRG*
[c] *Department of Radiology-Neuroradiology, Klinikum RWTH, Aachen, FRG*
[d] *Department of Anatomy, Klinikum RWTH, Aachen, FRG*
[e] *Department of Neurology, Heidelberg, FRG*

Accepted for publication: 8 August 1994

**Abstract**

Somatosensory evoked potentials (SEPs) to median nerve and finger stimulation were analyzed by means of spatio-temporal dipole modelling combined with 3D-NMR tomography in 8 normal subjects. The early SEPs were modelled by 3 equivalent dipoles located in the region of the brain-stem (B) and in the region of the contralateral somatosensory cortex (T and R). Dipole B explained peaks P14 and N18 at the scalp. Dipole T was tangentially oriented and explained the N20-P20, dipole R was radially oriented and modelled the P22. The tangential dipole sources T were located within a distance of 6 mm on the average and all were less than 9 mm from the posterior bank of the central sulcus. In 6 subjects the tangential sources related to finger stimulation arranged along the central sulcus according to the known somatotopy. The radial sources did not show a consistent somatotopic alignment across subjects. We conclude that the combination of dipole source analysis and 3D-NMR tomography is a useful tool for functional localization within the human hand somatosensory cortex.

*Keywords:* Early SEPs; Somatotopy; Somatosensory cortex; Dipole source analysis; 3D-NMR tomography

## 1. Introduction

The somatosensory representation of the digits in the primary human somatosensory cortex has been demonstrated first by electrical stimulation of the cortical surface (Penfield and Boldrey 1937) and later by electrocorticographically recorded somatosensory evoked potentials (Woolsey et al. 1979). More recently, the mapping of scalp recorded SEPs has shown a somatotopic arrangement of some potential fields (Duff 1980; Deiber et al. 1986). However, localization studies based on amplitude mapping may lead to ambiguous results for various reasons: (1) the electrode which records the maximum amplitude does not need to be next to the source (Nunez 1981, 1990; Gloor 1985); (2) the scalp SEP reflects the superposition of several source activities from different locations in the brain (Allison et al. 1991; Hari 1991); (3) scalp potentials are distorted and attenuated by the resistive properties of the skull and scalp (Fender 1981; Nunez 1991).

During the last decade, methods of dipole source analysis have been developed to solve the problem of spatial and temporal overlap (Scherg and Von Cramon 1985; Scherg 1990; Fender 1991). Dipole source analysis is based on 2 assumptions: (1) Localized neuronal activity of a circumscribed brain region can be modelled by an equivalent dipole (Nunez et al. 1991). Each active and functionally distinct brain region must be modelled at least by one equivalent dipole which is fixed in position and orientation (Scherg 1990, 1992). (2) The effects of volume conduction are approximated by a 3-shell spherical head model to consider the different electrical conductivities of the brain, skull and skin (Fender 1991).

* Corresponding author. Tel.: -241-8089827; Fax: -241-8888444.


*SSDI* 0013-4694(94)00228-2

EEP 93575

The problem of computing the location, orientation and magnitudes of one or several equivalent dipoles from scalp recorded potentials or fields is called the inverse problem. If formulated by the infinitesimal Poisson equation, this problem is unsolvable in principle (Nunez et al. 1991). However, if the model is made discrete as expressed in the above approximations, the inverse problem becomes solvable provided that the number of active brain regions is less than the number of recording channels and that the time epoch which is subjected to spatio-temporal analysis contains enough distinct spatial information on the discrete equivalent generators with respect to the noise in the signals (Scherg 1992). The inverse problem then consists in finding an adequate number of equivalent dipoles and to determine their locations, orientations and dipole moments. The wave forms associated with the magnitudes of the dipole moment, the dipole source potentials, reflect the estimated compound source current of the brain tissue around each source dipole. The solution is found by an interative process optimizing the source parameters for a given number of sources (Scherg 1990; Van Oosterom 1991). To improve the localization and separation of sources, each source can be fitted within the epoch of its maximal activity while holding the other sources fixed (Scherg and Berg 1991).

Dipole analyses of magnetic and electric recordings of early median nerve responses have provided models of 1–3 sources (Baumgartner et al. 1991a; Buchner and Scherg 1991; Hari 1991; Franssen et al. 1992), in good agreement with results from epicortical recordings and the physiology of the somatosensory system (Allison et al. 1989, 1991). Dipole localization of somatosensory magnetic fields evoked by finger stimulation (Okada et al. 1984; Baumgartner et al. 1991b) was consistent with the somatotopic arrangement known from the cortical stimulation studies by Penfield and Boldrey (1937). These authors have also shown that the human hand area does not occupy more than 30 mm along the central sulcus. In view of this small extent, it was questionable whether source analysis of scalp SEPs could reveal the somatotopical organization, because the accuracy of source localization based on scalp potentials had been reported to be in the order of 10 mm at best (Cuffin et al. 1991). However, in a preceding study, we have demonstrated a localization accuracy in intra-individual replications of median nerve SEPs of better than 9 mm, and deviations of the mean localization from the central sulcus, as determined from 3D-NMR tomography, of not more than 6 mm on the average and 9 mm maximally (Buchner et al. 1994a).

To our knowledge, there has been no report of somatotopy and source localization based on scalp SEPs following finger stimulation and only one comparison of somatosensory evoked fields with 3D-NMR tomography which include not more than 3 subjects (Suk et al. 1991). The results of this study and the accuracy of our previous SEP localizations encouraged us to study somatotopy using localization of scalp SEPs following finger stimulation. The main aims of the present study were: (1) to evaluate if a consistent difference in source localization of the SEP could be found for the stimulation of the fingers I, III and V; (2) to validate the source localizations relative to the individual anatomy of the central sulcus as derived from 3D-NMR tomography; and (3) to study a larger number of subjects using recordings with a dense array of 64 scalp electrodes.

## 2. Material and methods

*Subjects*

SEPs and 3D-NMR tomography were obtained from 8 normal right handed subjects, aged 22–39 years, 3 fe-

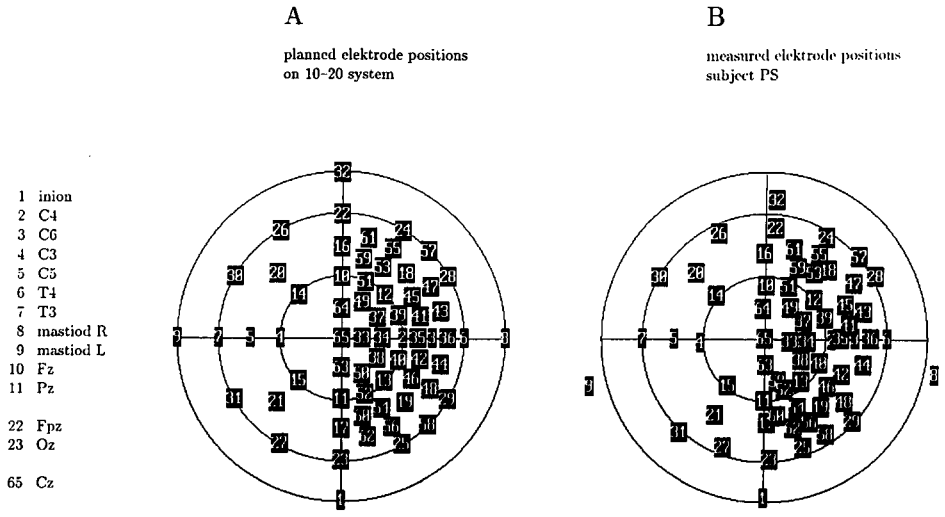


Fig. 1. Electrode locations shown in a top meridian projection around Cz (no. 65). A: planned locations on the basis of the 10–20 system. B: measured locations using 3D-NMR and back projection onto the best fitting sphere, subject PS.

males, 5 males. The subjects received 5–10 mg diazepam intravenously to reduce muscle artifacts during SEP recordings. All subjects gave their informed consent.

*SEP recording*

The median nerve at the left wrist was stimulated using constant current square wave pulses of 0.2 msec duration with a repetition rate of 3.1/sec and an intensity of twice the motor threshold of the thenar muscles. Fingers I, III and V of the left hand were stimulated separately using metallic bands fixed at the first and third interphalangeal joint. Stimulus intensity was set to twice the sensory threshold. SEPs were recorded from 65 scalp electrodes against a reference at Cz (Fig. 1). Electrodes were spaced more densely over the contralateral, right hemisphere. To record the small fields of the early SEPs, an interelectrode spacing of less than 3 cm is required for an accurate spatial sampling (Spitzer et al. 1989; Gevins et al. 1990). SEPs were sampled with 256 points over a 100 msec pre- and 100 msec poststimulus period. Recording bandpass was set to 5–250 Hz on the two 32-channel Nicolet SM 2000 amplifiers. Four replications of 1500 sweeps were averaged for each finger and median nerve stimulation using the Scan system (NeuroScan, Herndon, VA). After SEP measurements, the position of each electrode was marked by replacing it with a small wooden disk. Disks had a 3 mm hole filled with fat to visualize the position on the 3D-NMR.

*NMR acquisition*

NMR was performed after the SEP recording on the same day using a 1.5 T superconducting magnet and a circular polarized head coil. After parallel alignment of the interhemispheric plain of the brain with the sagittal imaging plain, a strongly T2-weighted gradient echo pulse sequence (fast-low-angle-shoot) was applied. For all NMRs the technical factors were: 50 msec repetition time, 5 msec echo time, 40° flip angle, one excitation, 30 cm field of view, 256 by 256 image matrix. This resulted in 128 continuous slices with a thickness of 1.56 mm and a pixel size of 1.1 mm.

*Data preprocessing*

NMRs were read into a system of computer assisted surgery (CAS), a image processing workstation and displayed in pseudo-3D view. The application of the CAS system for NMR evaluation has been discussed in detail elsewhere (Adams et al. 1990; Laborde et al. 1992). A surface reconstruction of the head was done for optimal visualization of the positions of the electrode markers (Fig. 2). The x-y-z coordinates of these markers were written to a file and transferred to a PC. A separate PC program was used to find the sphere best fitting the 3D electrode cloud (Law and Nunez 1991). The center of the sphere, its radius and the radial distances of the electrode positions from the center were computed in NMR coordinates. For source analysis, a coordinate system was defined that related closely to the standard 10–20 system of electrode placement: The z-axis was defined along the vector connecting the center of the sphere and the Cz electrode, the electrode at the inion (no. 1) then defined the y-z plane. Thus, the y-axis pointed anteriorly towards Fpz, and the x-axis laterally towards T4. Finally, electrodes were projected onto the fitted sphere and the according polar coordinates were

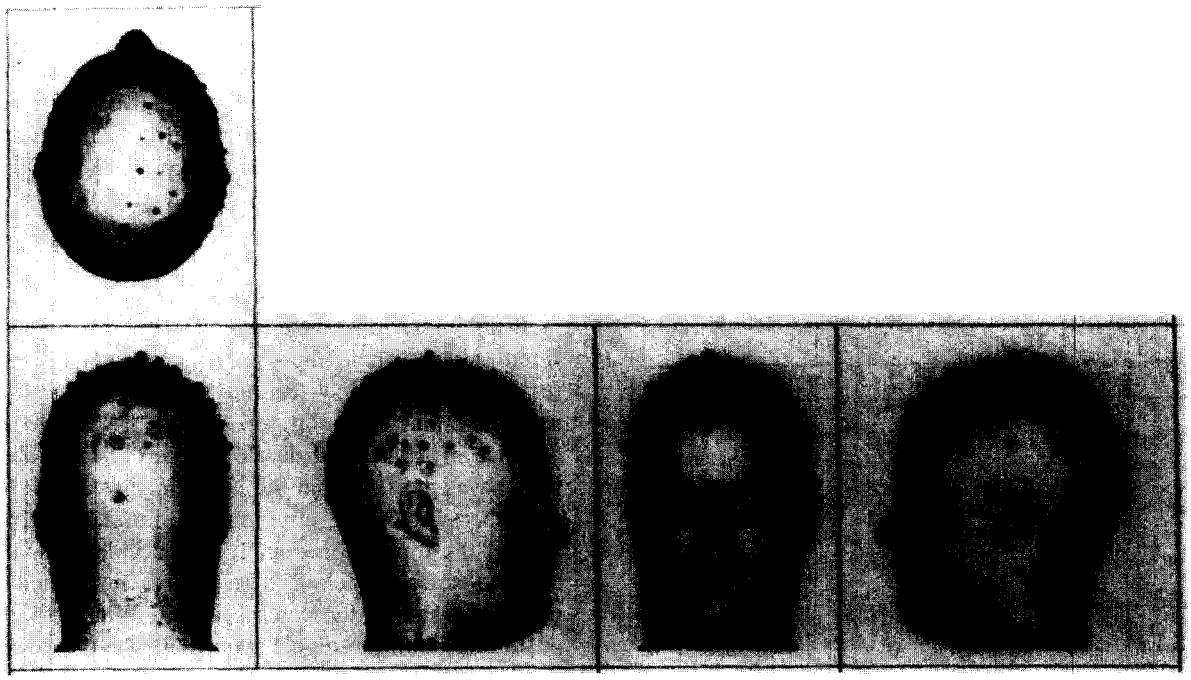

Fig. 2. 3D surface reconstruction of the NMR with electrode markers, subject MH.

input into the BESA program (Brain Electric Source Analysis, NeuroScan, Herndon, VA) for further processing.

Signals were baseline corrected by subtracting the mean signal from −100 to 0 msec and digitally filtered (high-pass: 20 Hz, 6 dB/oct, forward filter, and 250 Hz, 24 dB/oct, zero phase shift) in order to enhance the signal-to-noise ratio and to reduce the overlap of low frequency EEG components. This overlap, if not filtered out, can lead to substantial dipole mislocation. Also, most of the energy of the early SEPs is contained in this frequency band (Lüders et al. 1986). The average referenced data from −40 to 40 msec were retained for the BESA source analysis. Fig. 3 shows representative median nerve SEPs.

Signal epochs for source analysis were defined on the basis of the global field power (GFP; Lehmann 1987). Two epochs were defined: (1) between the minima of GFP before and after the P14, and (2) between the minima of GFP before and after the N20 and P22 (Fig. 3). Signal-to-noise ratio was computed for each channel by dividing the root mean square (RMS) amplitude in these epochs by the RMS amplitude of the prestimulus interval (−100 to 0 msec). Channels containing a noise amplitude of more than twice the median noise amplitude in the data set were excluded if there was a signal-to-noise ratio of less than 2 in the second epoch defined by the GFP. This resulted in the exclusion of maximally 3 electrodes in the case of median nerve and maximally 6 in the case of finger stimulated SEPs.

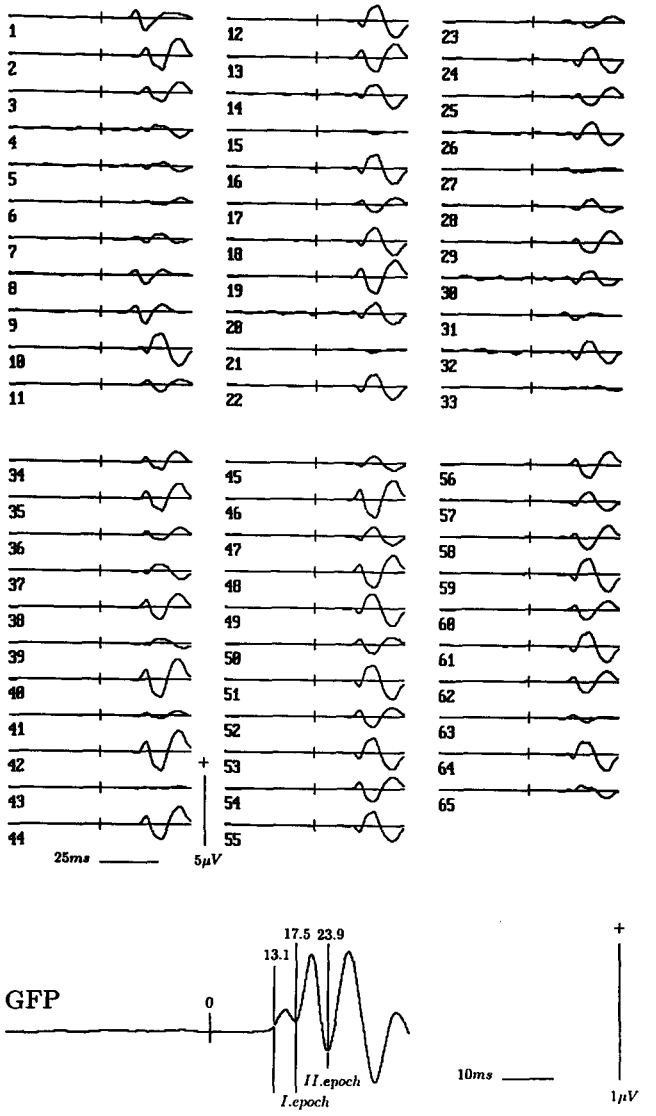


Fig. 3. Median nerve SEPs and GFP, 6000 averages, subject PS.

*Source analysis*

An approximated 3-shell head model was used to obtain an independent multiple dipole model for each SEP data set (Scherg and Von Cramon 1985, 1986; Fender 1991). A consistent strategy was applied for dipole localization of median nerve and finger stimulated SEPs (Fig. 4): (1) A regional dipole source, consisting of 3 orthogonal co-located dipoles explaining the 3-dimensional current flow of the surrounding brain region (Scherg 1990), was fitted to the first epoch as defined by the GFP. (2) A second regional dipole source was fitted to the second epoch, while the location of the first regional dipole source was held constant. (3) The orientation of the first dipole of each regional dipole source was rotated to explain the total current flow at the time of maximal activity of the regional dipole source in its respective epoch. The second and third dipoles of the first dipole source and the third dipole of the second regional dipole source were switched off, because they consistently showed little activity after this rotation. (4) The orientation and location of the remaining two dipoles of the second regional dipole source were fitted independently during the second epoch while holding constant dipole one of the first regional source.

The resulting model consisted of 3 dipole sources: The first (B = brain-stem) at the lower half of the head model explained the activity around 14 msec. The second (T = tangential) and third (R = radial) dipoles at the upper right quadrant of the head model explained the activities from around 18 to 25 msec.

*Comparison of NMR and source location*

Dipole locations were scaled with the radius of the fitted sphere. Then, dipole and sphere data were transferred into the CAS system, transformed into NMR coordinates and displayed on top of the NMR images. The distance of the second dipole source (T) from the central sulcus was defined from the NMR images as follows (Fig. 6): Spheres of 3 mm, 6 mm and 9 mm radius were drawn around the dipole location. It was decided visually from the CAS screen which of these spheres intersected with the posterior bank of the central sulcus. With respect to the position of the third dipole source (R), we only determined whether the location was anterior or posterior relative to the central sulcus.

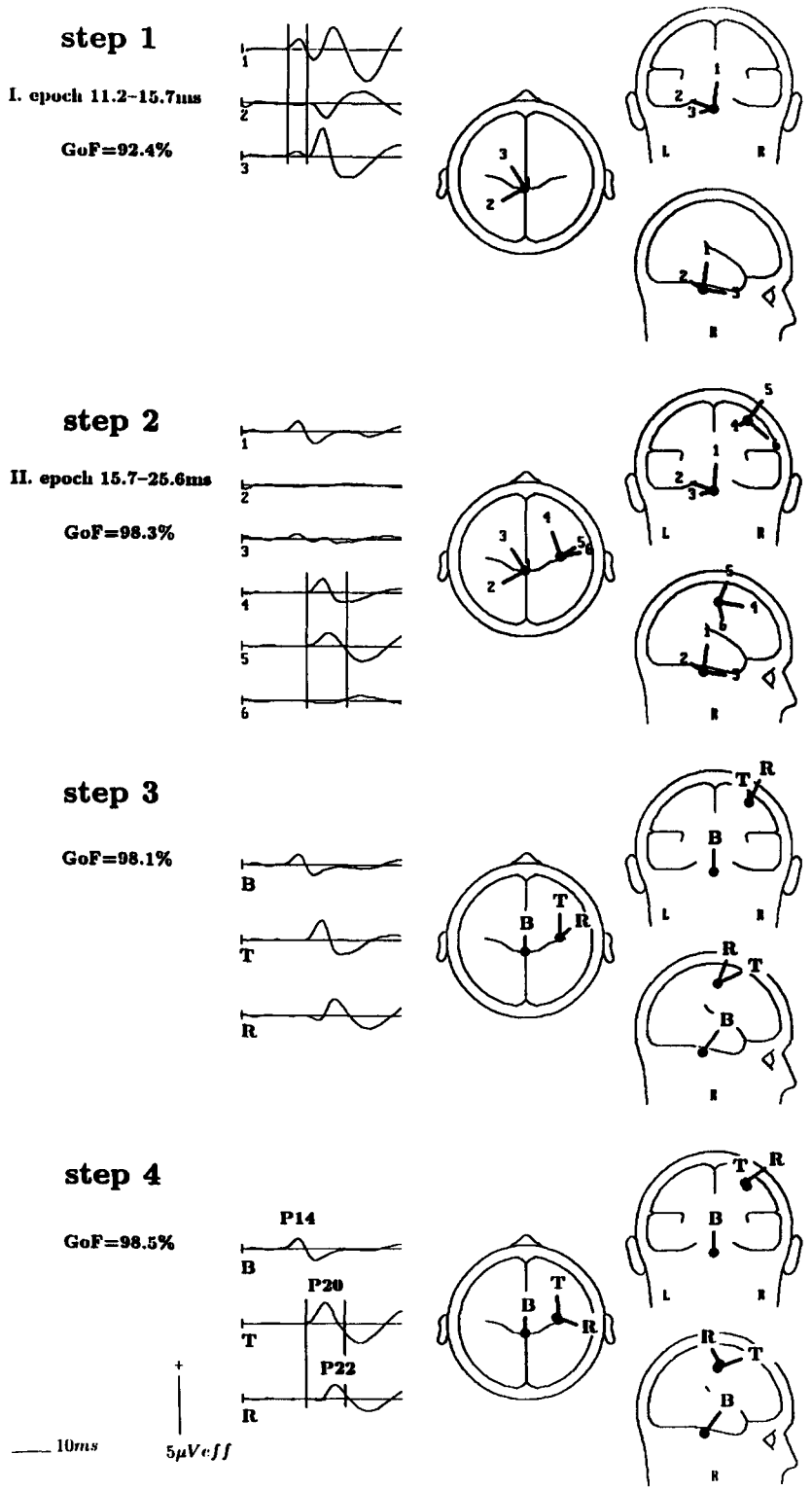


Fig. 4. Strategy of source analysis, data from subject IL. Locations and orientations of the dipole sources within the spherical head model are depicted in 3 projections: top, rear and lateral from right. The wave forms depict the magnitudes of the best fit source current of each dipole over time. Step 1: first regional dipole source fitted in epoch I defined by the GFP (dipoles 1–3). Step 2: second regional dipole source fitted in epoch II defined by the GFP, dipoles 1–3 held constant. Step 3: orientation of dipole 1 adjusted to fully explain N14. Dipoles 2–3 and 6 were switched off because of showing minimal activities in epochs I and II. Dipoles relabeled (B, T, R). Step 4: orientations and locations of the tangential cortical dipole (T) and the radial cortical dipole (B) source were fitted in epoch II. Dipole B (brain-stem) held constant. GoF = goodness of fit (100 − residual variance).

## 3. Results

*Electrode positions and best fit sphere*

The positions of the electrodes are shown in Fig. 1 in a top meridian projection: (A) at the planned locations within the 10/20 electrode system, and (B) at the measured locations as projected onto the sphere in subject PS. The radius of the fitted spheres ranged from 87.1 to 94.5 mm. The average of the radial deviation of all electrodes from the sphere ranged from 3.7 to 5.4 mm. The average of the radial deviation of electrodes above the stimulated, right hemisphere ranged from 2.0 to 4.2 mm. The electrode no. 1 at the inion, no. 22 at Pz and no. 32 at the nasion were markedly outside of the sphere. The temporal electrode nos. 5, 6, 7, 33 and 36 were markedly inside of the sphere. The electrode nos. 30 and 31 on the left side were further inside than the corresponding electrode nos. 28 and 29 on the right, because the center of the spheres was shifted 2 mm to the left of the interhemispheric plane on the average. This asymmetry was due to the attempt of the least squares fit to best match the more planar aspect of the right side of the head which was covered by the majority of the electrodes.

*Fitting and location of dipole sources*

Source analysis was performed for all data sets, except for the finger V SEPs of subject SS because of low signal-to-noise ratio. Two regional dipole sources were found to explain more than 95% of the variance in all data sets (Fig. 4, step 2). This very simple source model separated two active brain regions, one at the lower half of the head model and the other at its upper right. When the orientation of the first regional source was optimized, more than 90% of the activity in the first epoch was represented by its first dipole. Dipoles 2 and 3 were not needed to explain the data. Hence, they were switched off for further analysis, and the first dipole (B) was held constant to extract the N14-P18 complex from the data, because its activity persisted throughout both epochs.

When the orientation of the second regional source was optimized during the second epoch, less than 10% of its activity was represented by the third dipole of this regional source. Hence, this dipole was switched off for further analysis. This reduction to a total number of 3 dipoles did not substantially decrease the data variance explained by the model. The last step of computing resulted in the spatial separation of the tangential (T) and radial (R) dipoles of the second regional source located at the upper right of the head model.

Both for the median nerve and the finger stimulated SEPs, the resulting source model of 3 dipoles (B, T, R) showed activity patterns which contributed significantly to the scalp potentials. This model was found consistently in all but two data sets. In two cases of finger V SEPs (subjects AO and FL) no clear source activity was seen for the first dipole (B). This source at the lower half of the sphere explained 81.4–94.5% of the variance in the first epoch in the case of median nerve stimulation and 55.0–

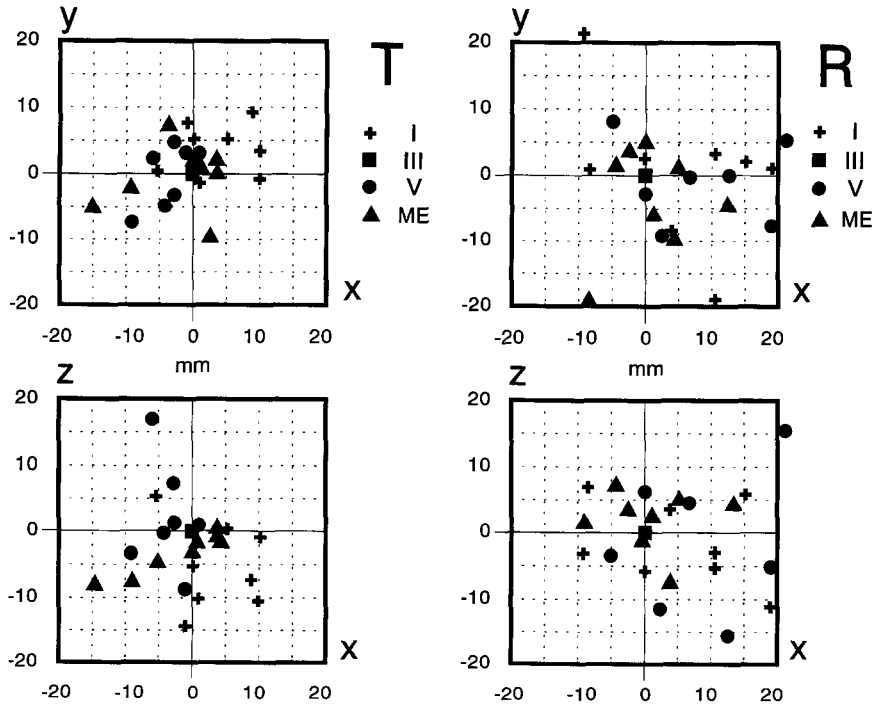


Fig. 5. Distance of the dipole sources of median nerve and finger I and V SEPs from the sources of finger III SEPs in the BESA coordinate system: x-axis towards the right ear, y-axis towards Fpz, z-axis connecting the center of the sphere and Cz. A: tangential source (T). B: radial source (R). The tangential sources show a somatotopical arrangement, while the radial source do not show a consistent pattern of localization.

92.0% (median 71.2%) in the case of finger stimulated SEPs. The orientation of dipole B pointed rostrally and towards the activated right hemisphere. Dipoles T and R were located in the region of the central sulcus contralateral to stimulation. Dipole T showed an almost tangential orientation while the orientation of the dipole R was predominantly radial. All 3 sources showed substantial overlap of activity during the second epoch (Fig. 4), ranging from about 16 to 24 msec in the case of median nerve stimulation and from 18 to 26 msec in the case of finger stimulation. The dipole model explained 90.7–98.7% (median 96.9%) of the variance in the second epoch, 96.9–98.7% in the case of median nerve stimulation, 90.7–98.2% in finger I stimulation, 92.3–97.3% in finger III, and 92.3–97.7% in finger V.

Source locations, orientations and wave forms were highly reproducible when fitting split-half subaverages of 3000 sweeps. The 3D distance of the split-half locations from the locations computed using the total 6000 averages served as an indicator for the reliability of source localization. Dipoles B had a mean 3D deviation between data sets of 8.7 mm (maximal 15.2 mm). Dipoles T had a mean 3D deviation of 3.2 mm (maximal 5.8 mm), and dipoles R a mean 3D deviation of 5.3 mm (maximal 8.7 mm).

*Spatial configuration of dipole sources*

Locations of the cortical sources T and R computed for median nerve and finger I and V SEPs are shown in Fig. 5 with respect to their location following finger III stimulation

Locations of the tangential sources are shown in Fig. 5A. Relative to finger III, finger I sources located more towards the right ear (x-axis), more frontally (y-axis) and more caudally in 6 of the 8 subjects. Finger V sources located more medially than finger III sources in 6 of 7 subjects, and more rostrally (z-axis) in 4 of 7 subjects. The location of the median nerve dipoles T relative to finger III was inconsistent along the x- and y-axis, but more caudally (z-axis) in 7 of 8 subjects.

Locations of the radial cortical sources are shown in Fig. 5B. A consistent pattern was found neither for the median nerve nor for the finger I and V dipoles as compared to the finger III dipole locations.

Comparing the relative locations of dipoles T and R of median nerve and finger stimulated SEPs, there was a clear tendency of the radial source to locate more towards the right ear (larger x, 23 of 31 sources) and more superficial (larger eccentricity, 25 of 31 sources). A consistent pattern was not obtained along the y-axis (occipital to frontal) and the z-axis (rostral to caudal). The average depth of the sources below the fitted sphere was 31.2 mm (S.D. 5.0 mm) for dipole T and 26.4 mm (S.D. 6.8 mm) for dipole R.

*Dipole location relative to anatomy*

The locations of the tangential and radial sources along the central sulcus were evaluated from the CAS screen (Fig. 6). In Fig. 7, the locations of dipole T relative to the interhemispheric plane, the central sulcus and the pre- and post-central sulci are depicted for all subjects. The distance

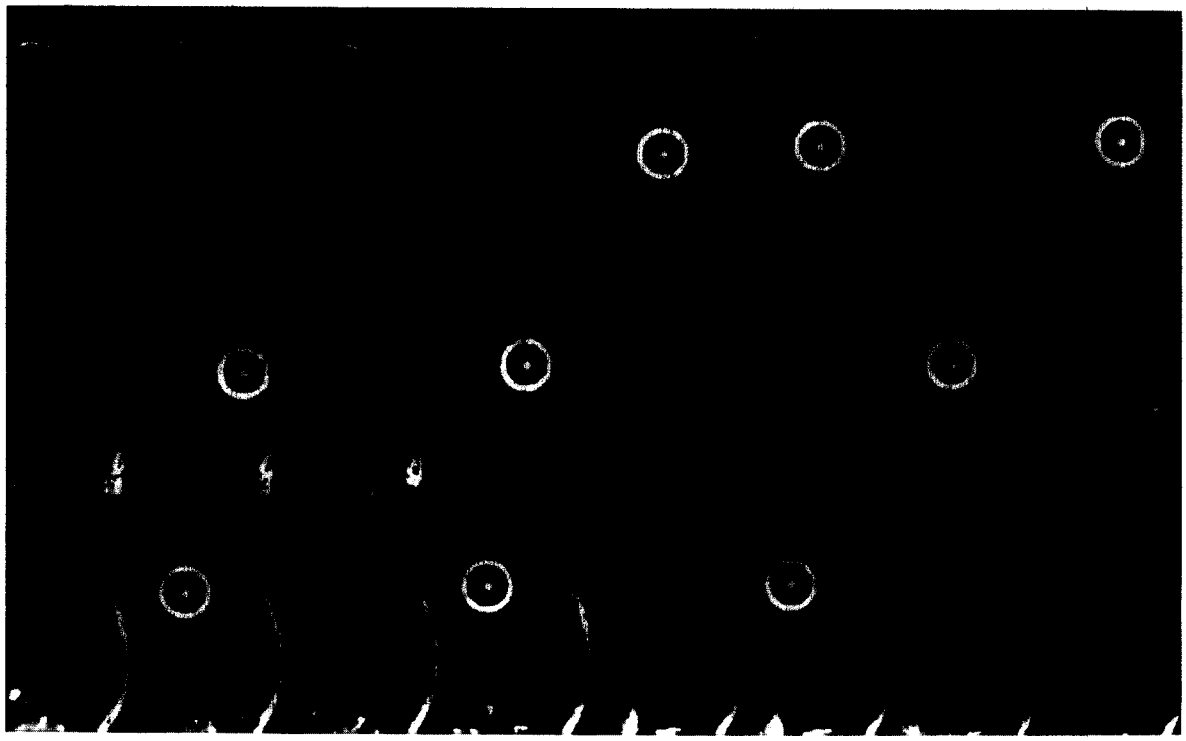

Fig. 6. NMR of subject MH showing the locations of the tangential source (cross within circle) of finger I, III and V SEPs. Note, that the estimated cortical representations of these fingers show a somatotopical arrangement.

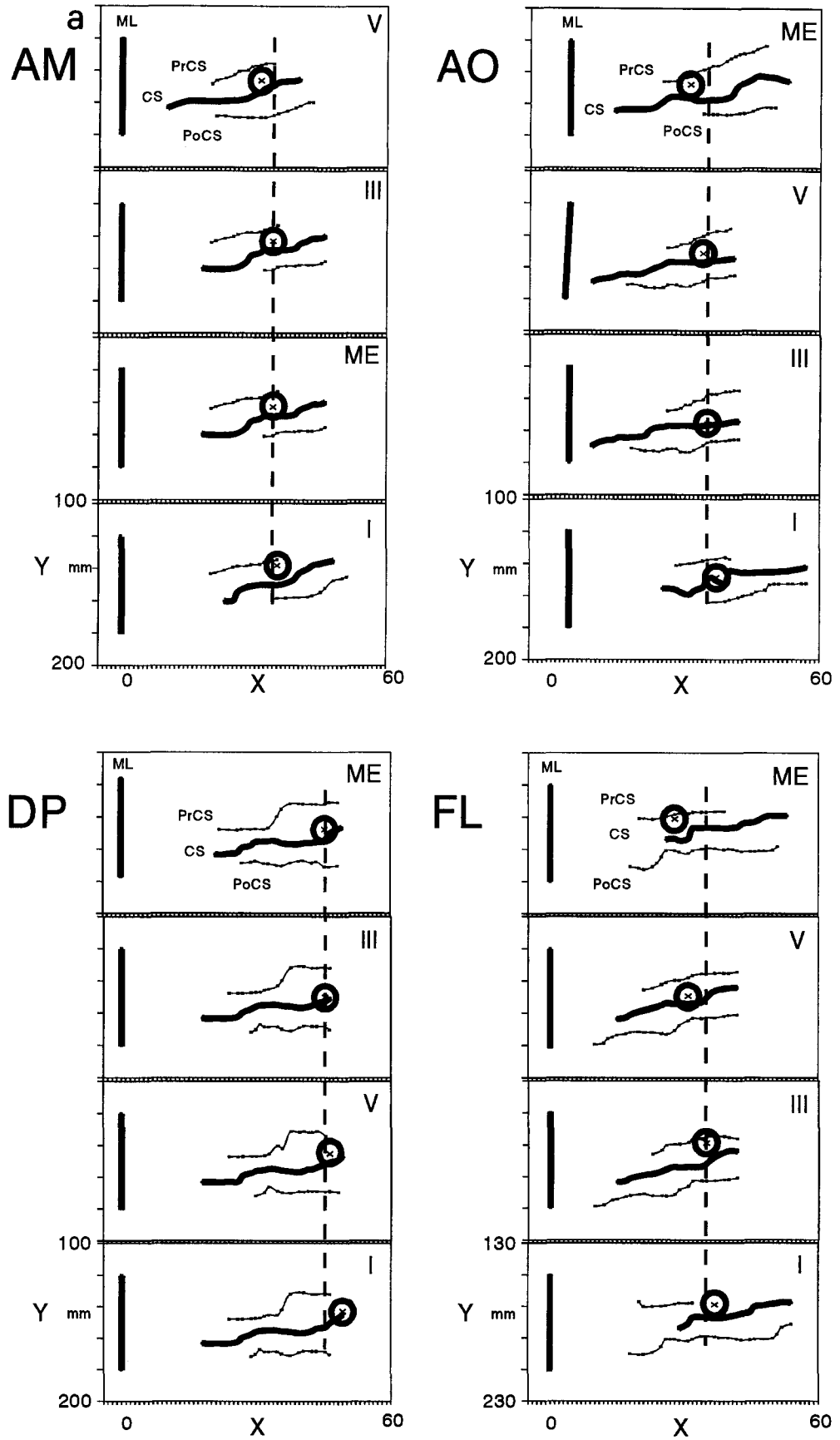


Fig. 7. Location of the tangential sources of the median nerve and finger SEPs relative to the central sulcus in each subject. The diagrams have been digitized from the axial NMR slices (x-axis pointing to the right, y-axis from frontal to occipital). Locations are plotted (cross and circle) relative to the interhemispheric plane (ML), central sulcus (CS), precentral sulcus (PrCS), and the postcentral sulcus (PoCS). The dashed vertical line marks the location of the finger III source on the x-axis. Circles were drawen to enhance visiblility, but do not indicate confidence limits.

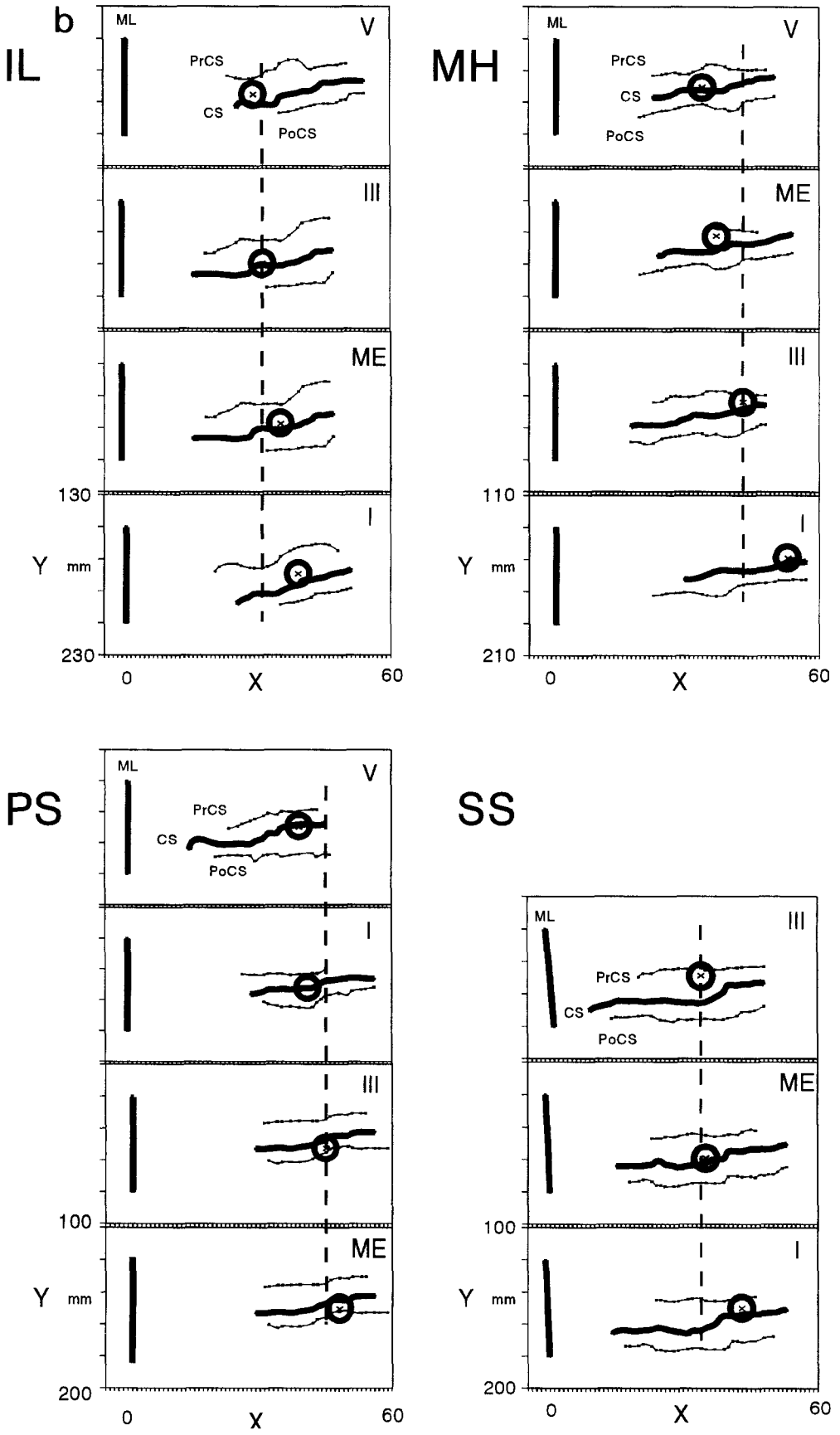


Fig. 7 (continued).

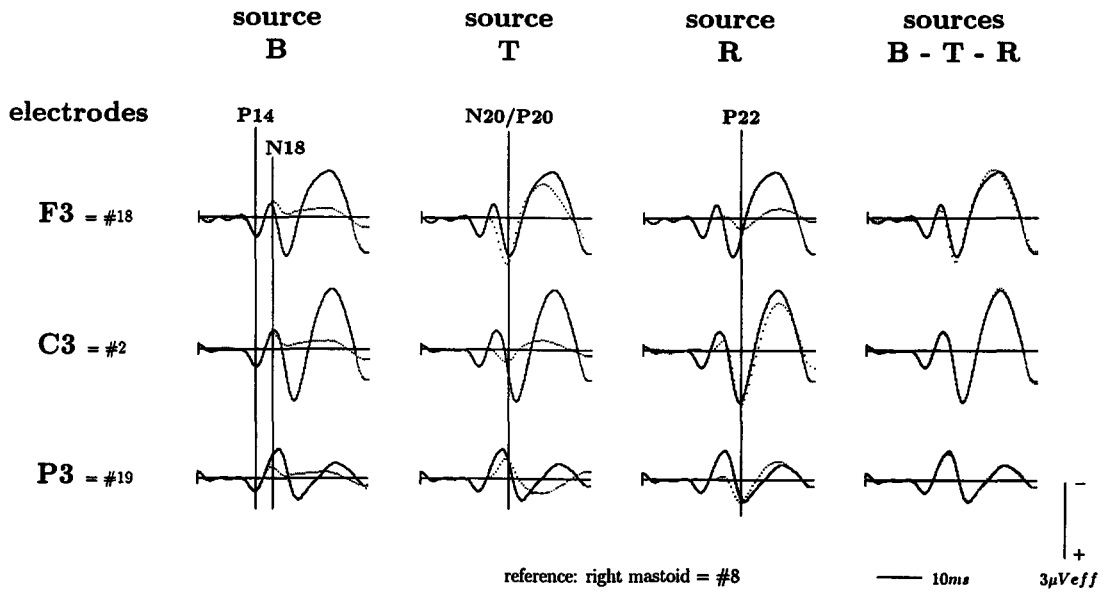


Fig. 8. Explanation of the phenomenon of overlap at 3 selected scalp electrodes (F3, C3, P3, subject IL). Recorded data (solid lines) and model (dotted lines) wave forms are compared using a left (contralateral) mastoid reference. The model wave forms depict the separate and summed contributions of the dipoles B, T and R to the electrodes. Source wave form B models the P14-N18 deflection, source wave form T contributes largely to the N20-P20 wave form and source R to the P22 wave form. Note that the peaks in scalp and source wave forms are not identical due to the different overlap of these activities at the 3 electrodes. For example, N20 and P20 latencies differ with respect to each other and to source wave form T.

of the dipole T from the posterior bank of the central sulcus was less than 3 mm in 14 stimulations, less than 6 mm in 10 stimulations and less than 9 mm in the remaining 8 cases. The tangential dipole located between 28 and 48 mm (median 35 mm), and the radial dipole between 32 and 53 mm (median 37 mm) laterally from the interhemispheric plane. The radial dipole located in front of the central sulcus in 9, within the sulcus in 10 and behind in 9 stimulations. In two data sets locations could not be determined.

In 6 subjects, the tangential dipole located along the central sulcus in the order of fingers V, III and I from medial to lateral. In subject PS the locations of fingers I and III, and in subject DP the locations of fingers III and V were reversed. The tangential median nerve source located between fingers I and V in 5 subjects. For the radial dipole, a consistent location pattern was not found.

We also computed the distance of tangential source (T) location from the central sulcus for median nerve SEPs using the planned electrode positions. In 2 subjects the accuracy of localization was not affected by the imprecise electrode locations. However, in 6 subjects the distance of the equivalent dipole from the central sulcus increased by 3–9 mm.

Three subjects (AM, MH, IL) were involved in the previous studies (Buchner et al. 1994a,b) and their median nerve SEPs and the NMR acquisitions were replicated in this study. Between these independent replications, the locations of the T dipole varied between the measurements by less than 6 mm in each subject.

In subject IL simultaneous electric and magnetic recordings of median nerve and finger stimulated SEPs were performed. Both methods demonstrated the same somatotopic arrangement of the fingers. The electric T dipole and the magnetic dipole located less than 6 mm apart.

## 4. Discussion

This study presents the first detailed report of somatotopical functional localization of the human hand area based on dipole source analysis of scalp SEPs. Source localizations of the tangential cortical source were very close to the central sulcus in each of the 8 subjects and for each finger as revealed by individual 3D-NMR tomography. These findings support and extend a previous comparison based on single dipole localization of somatosensory evoked fields in 3 subjects (Suk et al. 1991).

Although consisting only of 3 dipoles and 3 source potential wave forms, our model explained a very large amount of the variance in the 64 scalp channels in each data set (median 96.9%). It separated 3 overlapping source activities from brain regions known to be involved in the generation of the early median nerve and finger SEPs. Onset and peak latencies of the source wave forms as well as the locations and orientations of the 3 dipoles (B, T, R) reflected the activation along major parts of the somatosensory system consistent with previous studies (Buchner and Scherg 1991; Franssen et al. 1992).

*Comparison of source and scalp potential wave forms*

The contribution of each source wave form to the potential wave forms at the scalp is illustrated in Fig. 8 for 3 selected electrodes. Dipole B, located in the region of the

brain-stem at the lower half of the head model, explained most of scalp potentials P14 and N18. There is evidence that P14 is generated at the level of the medial lemniscus (Desmedt 1988) and that other sources contribute to the scalp N18 as well (Desmedt and Cheron 1981; Mauguière et al. 1983a; Raroque et al. 1994). However, for physical reasons the biphasic far-field activity of dipole B may be largely due to or enhanced by the abrupt change of the volume conductor at the foramen magnum when the median nerve trunk enters the cranium (Lüders et al. 1983; Buchner et al. 1987). On the basis of such a mechanism, a biphasic wave shape is to be expected (Kimura et al. 1984).

In an earlier study using median nerve SEPs, a dipole source separate from dipole B and close to the thalamus was found. This source appeared to reflect the output from the thalamus into the thalamo-cortical pathway with an initial peak around 16 msec and a radial orientation (Buchner and Scherg 1991). Due to this orientation, a small error may be introduced in the localization of the more superficial cortical dipole R, if the deeper but almost parallel thalamic activity is not modelled. However, because this activity was very small at the scalp and because it could not be reliably located in most finger SEPs, we did not include a thalamic source in the present model.

The second, tangential dipole source (T) explained the initial activity of the somatosensory cortex. This source was tangentially oriented and closely modelled the N20-P20 peaks at the scalp. Orientation and location of this source suggest an origin at the posterior bank of the central sulcus. This interpretation is in agreement with a variety of studies using EEG scalp recordings, MEG and electrocorticography (for review see Desmedt 1988; Allison et al. 1991; Baumgartner et al. 1991a,b).

The tangential dipole activity was followed by an almost radially oriented source activity (R), reflecting the central P22 peak on the scalp. The orientation and more superficial location are consistent with a generation at the cortical surface, i.e., at the crown of the central gyrus. There is an ongoing discussion whether P22 originates precentrally (area 4) or postcentrally (area 1) (Mauguière et al. 1983b, 1991; Deiber et al. 1986; Desmedt et al. 1987; Desmedt 1988; Hashimoto et al. 1990; Allison et al. 1991). Our results cannot contribute to this discussion, because the localization of the radial dipole R scattered equally to both sides of the central sulcus. To some extent, the observed scatter of the radial dipole location may be due to the simplified model of 3 equivalent dipoles and the severe overlap of at least two cortical soures (see discussion below).

*Source location with respect to NMR images and somatotopical organization*

The observed locations of the tangential dipoles along the central sulcus were in good agreement with the somatotopic arrangement of primary cortical finger representations (Penfield and Boldrey 1937; Merzenich et al. 1978; Allison et al. 1991). Such functional areas have a spatial extent of typically one to several square centimeters. Their size can roughly be estimated from the magnitude the tangential equivalent dipole obtained by magnetic measurements (Lopes da Silva et al. 1991). A size of about 1.5 $cm^2$ has been calculated for the primary cortical activity of median nerve SEPs, and a size of 0.5 $cm^2$ for the finger SEPs. This is in line with a maximal depth of the central sulcus at the hand area of 24 mm and an extent of the receptive fields along the central sulcus of 9 mm for median nerve and 3 mm for finger stimulation (Buchner et al. 1994b).

Considering, the cumulative thickness of the scalp, skull, CSF and dura of about 14–17 mm, the observed depth of 31 mm below the head surface is consistent with a location of the tangential SEP dipole close to the center of the active source area at the posterior wall of the central sulcus. Thus the dipole may reside at some "center of gravity" within the active source region (Nunez 1990; Scherg 1990). However, incompletely modelled overlaps from other generators, inaccuracies of the head model and noise in the data may lead to systematic errors of this ideal location. Also, there might be a shift of the "center of gravity" due to an overlap of the receptive fields (Merzenich et al. 1983). For this reason, dipole source location is not identical to the anatomical location of a certain functional area of the cortex.

In our study, however, these factors and the modelling errors were small enough to allow for the detection of the somatotopical order of the *tangential* source activity along the central sulcus. This order was reversed only in two subjects and only with respect to two fingers.

Using the CAS system, we were able to evaluate the locations of the tangential dipoles along the central sulcus, and distances from the posterior bank of the central sulcus within the NMR images (Figs. 6 and 7). Considering all 32 conditions of median nerve and finger stimulations, distances were less than 3 mm in 14, less than 6 mm in 10, and less than 9 mm in 8 conditions. This replicates results of a previous study of 39 right and left median nerve SEPs recorded with fewer (32) electrodes from 20 subjects. In this study distances from the central sulcus were less than 3 mm in 15, less than 6 mm in 10 and less than 9 mm in 14 instances (Buchner et al. 1994a). There was a tendency of the sources to locate anteriorly with respect to the central sulcus. This, to our opinion, is a systematic error due to the spherical head model not taking into account the more ellipsoid geometry of the heads (Law and Nunez 1991). However, this and the method used to fit the sphere to the individual heads can only evaluate once more realistically shaped models are available for comparison.

Location accuracy could not be tested against the NMR with respect to the depth of the source, because there is no anatomical landmark indicating the "center of gravity" in this direction. However, the average depth of 3.1 cm of the

tangential dipole from the fitted sphere (about 1.6 cm from the cortical surface) was consistent with the anatomy of the central sulcus. Furthermore, the comparison of the locations of the tangential and radial cortical dipoles showed a consistently more superficial location for the radial dipole. It was the depth direction or eccentricity, respectively, along which the most obvious relative differences were found for these two sources. However, the accuracy of the absolute estimates of source depth from EEG data should improve, if the thicknesses of the shielding skull and scalp layers will be considered on an individual basis in the future.

There was no consistent localization of the *radial* source neither in respect to somatotopy nor relative to its location in front or behind the central sulcus. From simulations (e.g., Scherg 1990), it is obvious that location and orientation of a superficial dipole interact, because a small shift in position can be largely compensated by a corresponding change in orientation to yield an almost identical scalp potential distribution. For this reason, the scatter of the radial source to either side of the central sulcus is plausible.

Earlier studies using scalp potential mapping demonstrated a somatotopic arrangement of the P22 but not of the N20-P20 field (Duff 1980; Deiber et al. 1986) which partly reflects our tangential dipole T. This discrepancy was mainly caused by the selection of the apparently most radial field pattern by Deiber et al. (1986), presenting a constraint on the orientation which we did not impose on the radial dipole (R). Franssen et al. (1992) also used a constraint on the orientation of the radial dipole and found a more medial location of the radial relative to the tangential dipole as compared to our study. Recomputations of our data using this strategy also resulted in a more medial location of the radial source. Hence, this shift in location appears to be mainly a consequence of the imposed constraints. Our presented strategy tried to avoid such constraints without definitive anatomical foundation. Subdural and epicortical recordings have revealed a more medial location of the radial field pattern (Sutherling et al. 1988; Allison et al. 1989). This discrepancy may partly be explained by the shortcomings of the spherical head model used in this and the study of Franssen et al. (1992) based on an approximation of the 3-shell head model according to Ary et al. (1981). Also, there was an asymmetry of the fitted sphere as viewed from the hand area with respect to the location of the electrodes at the vertex and at the temporal lobe where electrode were further inside. In addition, the skull is thinner at the temporal bone than in the frontal or occipital region (Myslobodsky et al. 1991). These factors make an apparent shift of the radial dipole towards the lateral plausible.

*Accuracy of dipole source modelling*

Dipole models are only crude representations of the underlying physiological processes, because: (1) each equivalent dipole may represent a complex and spatially extended source region (see discussion above), (2) the spherical head model is a simplified approximation to the geometry and resistive properties of the head tissues, and (3) spatial resolution is limited because of the limited number of recording channels (Nunez 1981; Fender et al. 1987; Spitzer et al. 1989; Gevins et al. 1990). In addition, closely located generators with source activities oriented in opposite directions, e.g., from both sides of a sulcus, may partially cancel out (Nunez 1981; Jayakar et al. 1991) or lead to the mislocation of their equivalent dipole (Scherg and Berg 1991). A more complex source model can cause ambiguities in computing the inverse solution (Achim et al. 1988; Cuffin et al. 1991). For instance, there is evidence for not modelled additional generator activity contributing to the SEPs after 22 msec post stimulus (García-Larrea et al. 1992).

However, our spatio-temporal dipole model of 3 sources (B, T, R) proved highly reliable and consistent between subjects. In fact, it was necessary to use this spatio-temporal model to separate the strong overlap of the source activity of the brain-stem and of the predominantly tangential and radial source activities in the region of the central sulcus (Fig. 4, step 4). The peaks of the latter cortical activities reflect N20/P20 and P22 but they are not precisely identical in latency with these scalp deflections (Fig. 8) (Franssen et al. 1992). Hence, mapping and single dipole localization may be misleading because these methods are not capable of resolving such overlap. Indeed, in several cases the single dipole fit at the peak of N20 deviated by several centimeters from the spatio-temporal solution.

The complexity of the spatio-temporal dipole model, especially the non-linearity of the source location parameters, prohibits the simple estimation of a confidence interval for the coordinates of each dipole (Mosher et al. 1993). However, when we independently relicated dipole localization over split-halfs of the total 6000 averages for each condition and subject, we found a mean replication error in localization of 3.2 mm and a maximal error of 5.8 mm. This confirmed results of our previous study which used only 32 scalp channels and showed a replication error across 4 subaverages in the order of 6 mm (Buchner et al. 1994a). The magnitude of error in the present study is within expected range considering the large number of channels and the fairly shallow depth of the tangential SEP dipole (Cuffin et al. 1991). Taking into account these results and the observed close distances of fingers I, III and V tangential dipole locations to the central sulcus, as validated independently by 3D-NMR tomography, we can estimate the 95% confidence interval to be in the order 5–6 mm for the localization of the tangential SEP dipole using our 64-channel scalp montage and the projection of the 3D electrode locations onto the best fitting sphere. Compared to this measure, the observed distances between source locations of fingers I and III (median 11.4 mm,

range 3.4–15.7 mm), III and V (median 9.6 mm, range 6.7–12.1 mm) were significant.

Our source locations could be not validated directly lacking an independent reference as given, for example, by stimulation of implanted electrodes (Cuffin et al. 1991). However, we were able to provide a comparison with the individual anatomical location of the central sulcus as based on 3D-NMR in all subjects. This comparison indicated that EEG source localization, using 64 scalp channels, exhibits an accuracy close to that of present MEG systems (Cohen et al. 1990; Hari et al. 1991). Further evidence for the reliability of EEG source localization in the central area is coming from a recent study using simulaneous magnetic and electrical recordings of somatosensory evoked responses showing distances of less than 6 mm between EEG and MEG locations (Buchner et al. 1994).

We suggest that 3 factors are responsible for this accuracy found consistently in our two independent studies. First, the precise 3D measurement of electrode positions with respect to the NMR images and their equivalent projection onto the surface of the best fitting sphere (Law and Nunez 1991; Lagerlund et al. 1993; Towle et al. 1993) provide a sufficiently accurate spatial reference within the tangential plane of the source. Second, the central sulcus resides in a favorable region of the brain in which the sources are not too deep below the surface and for which the best fitting sphere provides a reasonably good approximation. Third, the spatio-temporal multiple source model separated the overlapping activities from other brain regions.

## Acknowledgments

Supported in part by the Bundesministerium für Forschung und Technik – MEDWIS – Hybrider Konsiliar für die Neurowissenschaften and the Volkswagen Foundation.

## References

Achim, A., Richer, R. and Saint-Hilaire, J.M. Methods for seperating temporally overlapping sources of neuroelectric data. Brain Topogr., 1988, 1: 22–28.

Adams, L., Krybus, W., Meyer-Ebrecht, D., Rüger, R., Gilsbach, J.M., Moesges, R. and Schloendorff, G. Computer-assisted surgery. IEEE Comput. Graph. Appl., 1990, 10: 43–51.

Allison, T., McCarthy, G., Wood, C.C., Darcey, T.M., Spencer, D.D. and Williamson, P.D. Human cortical potentials evoked by stimulation of the median nerve. I. Cytoarchitectonic areas generating short-latency activity. J. Neurophysiol., 1989, 62: 694–710.

Allison, T., McCarthy, G., Wood, C.C. and Jones, S.J. Potentials evoked in human and monkey cerebral cortex by stimulation of the median nerve. Brain, 1991, 114: 2465–2503.

Ary, J.P., Klein, S.A. and Fender, P.H. Location of sources of evoked scalp potentials; correction of skull and scalp thickness. IEEE Trans. Biomed. Eng., 1981, BME-28: 447–452.

Baumgartner, C., Barth, D.S., Levesque, M.F. and Sutherling, W.W. Functional anatomy of human hand sensorimotor cortex from spatiotemporal analysis of electrocorticograhy. Electroenceph. clin. Neurophysiol., 1991a, 78: 56–65.

Baumgartner, C., Doppelbauer, A., Deecke, L., Barth, D.S., Zeitlhofer, J., Lindinger, G. and Sutherling, W.W. Neuromagnetic investigation of somatotopy of human hand somatosensory cortex. Exp. Brain Res., 1991b, 87: 641–648.

Buchner, H. and Scherg, M. Analyse der Generatoren früher kortikaler somatosensibel evozierter Potentiale (N. medianus) mit der Dipolquellenanalyse: erste Ergebnisse. Z. EEG-EMG, 1991, 22: 62–69.

Buchner, H., Ferbert, A., Brückmann, H. and Hacke, W. The subcortical generated somatosensory evoked potentials in non-cephalic, cephalic and anterior neck referenced recordings in a patient with a cervicomedullary lesion: a cue to the identification of the P14/N14 and N13 generators. J. Neurol., 1987, 234: 412–415.

Buchner, H., Adams, L., Knepper, A., Rüger, R., Laborde, G., Ludwig, I., Reul, J. and Scherg, M. Preoperative localization of the central sulcus by dipole source analysis of early somatosensory evoked potentials and 3-dimensional magnetic resonance imaging. J. Neurochir., 1994a, 80: 849–856.

Buchner, H., Fuchs, M., Wischmann, A.-H., Dössel, O., Ludwig, I., Knepper, A. and Berg, P. Source analysis of median nerve and finger stimulated somatosensory evoked potentials: multichannel simultaneous recording of electric and magnetic fields combined with 3D-MR tomography. Brain Topogr., 1994b, 6: 299–310.

Cohen, D., Cuffin, B.N., Yunokuchi, K., Maniewski, R., Purcell, C., Cosgrove, G.R., Ives, J., Kennedy, J.G. and Schomer, D.L. MEG versus EEG localization test using implanted sources in the human brain. Ann. Neurol., 1990, 28: 811–817.

Cuffin, B.N., Cohen, D., Yunokuchi, K., Maniewsi, R., Purcell, C., Cosgrove, G.R., Ives, J., Kennedy, J. and Schomer, D. Tests of EEG localisation accuracy using implanted sources in the human brain. Ann. Neurol., 1991, 29: 132–138.

Deiber, M.P., Giard, M.H. and Mauguière, F. Separate generators with distinct orientations for N20 and P22 somatosensory evoked potentials to finger stimulation. Electroenceph. clin. Neurophysiol., 1986, 65: 321–334.

Desmedt, J.E. Somatosensory evoked potential. In: T.W. Picton (Ed.), Human Event-Related Potentials. Handbook of EEG and Clinical Neurophysiology (Revised Ser.), Vol. 3. Elsevier, Amsterdam, 1988: 245–360.

Desmedt, J.E. and Cheron, G. Non-cephalic reference recording of early somatosensory potentials to finger stimulation in adult or aging normal man. Differentiation of widespread N18 and contralateral N20 from the prerolandic P22 and N30 components. Electroenceph. clin. Neurophysiol., 1981, 52: 553–570.

Desmedt, J.E., Nguyen, T.H. and Bourguet, M. Bit-mapped color imaging of human evoked potentials with reference to the N20, P22, P27 and N30 somatosensory responses. Electroenceph. clin. Neurophysiol., 1987, 68: 1–19.

Duff, T.A. Topography of scalp recorded potentials evoked by stimulation of the digits. Electroenceph. clin. Neurophysiol., 1980, 49: 452–460.

Fender, D.H. Models of the human brain and the surrounding media: their influence on the reliability of source localization. J. Clin. Neurophysiol., 1991, 8: 381–390.

Franssen, H., Stegeman, D.F., Moleman, J. and Schoobaar, R.P. Dipole modelling of median nerve SEPs in normal subjects and patients with small subcortical infarcts. Electroenzeph. clin. Neurophysiol., 1992, 84: 401–417.

García-Larrea, L.G., Bastuji, H. and Mauguière, F. Unmasking of cortical SEP components by changes in stimulus rate: a topograpic study. Electroenceph. clin. Neurophysiol., 1992, 84: 71–83.

Gevins, A., Le, J., Brickett, P., Costales, B., and Reuter, B. Beyond topographic mapping: towards functional-anatomical imaging with 124-channel EEGs and 3-D MRIs. Brain Topogr., 1990, 3: 53–64.

Gloor, P. Neuronal generators and the problem of localization in electroencephalography: application of volume conductor theory to electroencephalography. J. Clin. Neurophysiol., 1985, 2: 327–354.

Hari, R. On brain magnetic responses to sensory stimuli. J. Clin. Neurophysiol., 1991, 8: 157–169.

Hari, R., Hämäläinen, M., Ilmoniemi, R. and Lounasmaa, O.V. MEG versus EEG localization test. Ann. Neurol., 1991, 30: 222–223.

Hashimoto, S., Segawa, Y., Kawamura, J., Harada, Y., Yamamoto, T., Suenaga, T., Shigematu, K., Iwami, O. and Nakamura, M. Volume conduction of the parietal N20 potential to the prerolandic frontal area. Brain, 1990, 113: 1501–1509.

Jayakar, P., Duchowny, M., Resnick, T.J. and Alvarez, L.A. Localization of seizure foci: pitfalls and caveats. J. Clin. Neurophysiol., 1991, 8: 414–431.

Kimura, J., Mitsudore, A., Yamada, T. and Dickins, Q.S. Stationary peaks from a moving source in far-field recording. Electroenceph. clin. Neurophysiol., 1984, 58: 351–361.

Laborde, G., Gilsbach, J., Harders, A., Klimek, I., Nachtsheim, A. and Krybus, W. Computer assisted localizer for planning of surgery and intra-operative orientation. Acta Neurochir. (Wien), 1993, 119: 166–170.

Lagerlund, T.D., Sharbrough, F.W., Jack, C.R., Erickson, B.J., Strelow, D.C., Cicora, K.M. and Busacker, N.E. Determination of 10–20 system electrode locations using magnetic resonance imaging scanning with markers. Electroenceph. clin. Neurophysiol., 1993, 86: 7–14.

Law, S.K. and Nunez, P.L. Quantitative representation of the upper surface of the human head. Brain Topogr., 1991, 3: 365–371.

Lehmann, D. Principles of spatial analysis. In: A.S. Gevins and A. Rémond (Eds.), Methods of Analysis of Brain Electrical and Magnetic Signals. EEG Handbook (Rev. Series), Vol. 1. Elsevier, Amsterdam, 1987: 309–354.

Lopes da Silva, F.H., Wieringa, H.J. and Peters, M.J. Source localization of EEG versus MEG: empirical comparison using visually evoked responses and theoretical considerations. Brain Topogr., 1991, 4: 133–142.

Lüders, H., Lesser, J., Hahn, J., Little, J. and Klem, G. Subcortical somatosensory evoked potentials to medial nerve stimulalion. Brain, 1983, 106: 341–372.

Lüders, H., Dinner, D.S., Lesser, R.P. and Morris, H.H. Evoked potentials in cortical localization. J. Clin. Neurophysiol., 1986, 3: 75–84.

Mauguière, F. and Desmedt, J.E. Focal capsular vascular lesions can selectively deafferentate the prerolandic or the parietal cortex: somatosensory evoked potential evidence. Ann. Neurol., 1991, 30: 71–75.

Mauguière, F., Desmedt, J. and Courjon, J. Neural generators of N18 and P14 far-field SEPs. Electroenceph. clin. Neurophysiol., 1983a, 56: 283–292.

Mauguière, F., Desmedt, J. and Courjon, J. Astereognosis and dissociated loss of frontal or prietal components of somatosensory evoked potentials in hemispheric lesion – detailed correlations with clinical signs and computerized tomographic scanning. Brain, 1983b, 106: 271–311.

Merzenich, M.M., Kaas, J.H., Sur, M. and Lin, C.S. Double representation of the body surface within cytoarchitectonic areas 3b and 1 in "SI" in the owl monkey (*Aotus trivirgatus*). J. Comp. Neurol., 1978, 181: 41–74.

Merzenich, M., Kaas, J.H., Wall, J.T., Sur, M., Nelson, R.J. and Felleman, D.J. Progression of change following median nerve section in the cortical representation of the hand in areas 3b and 1 in adult owl and squirrel monkeys. Neurosience, 1983, 10: 639–665.

Mosher, J.C., Spencer, M.E., Leahy, R.M. and Lewis, P.S. Error bounds for EEG and MEG dipole source localization. Electroenceph. clin. Neurophysiol., 1993, 86: 303–321.

Myslobodsky, M.S., Coppola, R. and Weinberger, D.R. EEG laterality in the era of structural brain imaging. Brain Topogr., 1991, 3: 381–390.

Nunez, P.L. Electric Fields of the Brain. Oxford University Press, New York, 1981.

Nunez, P.L. Localization of brain activity with electroencephalography. In: S. Sato (Ed.), Magnetoencephalography (AdVances in Neurology, Vol. 54). Raven Press, New York, 1990: 39–65.

Nunez, P.L., Pilgren, K.L., Westdorp, A.F., Law, S.K. and Nelson, A.V. A visual study of surface potentials and laplacians due to distributed neocortical sources: computer simulations and evoked potentials. Brain Topogr., 1991, 4: 151–168.

Okada, Y.C., Tanenbaun, R., Williamson, S.J. and Kaufman, L. Somatotopic organization of the human somatosensory cortex revealed by neuromagnetic measurements. Exp. Brain Res., 1984, 56: 197–205.

Penfield, W. and Boldrey, E. Somatic motor and sensory representation in the cerebral cortex of man as studied by electrical stimulation. Brain, 1937, 60: 389–443.

Raroque, H.G., Batjer, H., White, Ch., Bell, W.L., Bowman, G. and Greenlee, R. Lower brain-stem origin of the medial nerve N18 potential. Electroenceph. clin. Neurophysiol., 1994, 90: 170–172.

Scherg, M. Fundamentals of dipole source potential analysis. In: F. Grandori, M. Hoke and G.L. Romani (Eds.), Auditory Evoked Magnetic Fields and Electric Potentials (Advances in Audiology, Vol. 6). Karger, Basel, 1990: 40–69.

Scherg, M. Functional imaging and localization of electromagnetic brain activity. Brain Topogr., 1992, 5: 103–112.

Scherg, M. and Berg, P. Use of prior knowledge in brain electromagnetic source analysis. Brain Topogr., 1991, 4: 143–150.

Scherg, M. and Von Cramon, D. Two bilateral sources of the late AEP as identified by a spatio-temporal dipole model. Electroenceph. clin. Neurophysiol., 1985, 62: 32–44.

Scherg, M. and Von Cramon, D. Evoked dipole source potentials of the human auditory cortex. Electroenceph. clin. Neurophysiol., 1986, 65: 344–360.

Spitzer, A.R., Cohen, L.G., Fabrikant, J. and Hallett, M. A method for determining optimal interelectrode spacing for cerebral topographic mapping. Electroenceph. clin. Neurophysiol., 1989, 72: 355–361.

Suk, J., Ribary, J., Cappell, T., Yamamoto, T. and Llinás, R. Anatomical localization revealed by MEG recordings of the human somatosensory system. Electroenceph. clin. Neurophysiol., 1991, 78: 185–196.

Sutherling, W.W., Crandall, P.H., Darcey, T.M., Becker, D.P., Levesque, M.F. and Barth, D.S. The magnetic and electric fields agree with intracranial localizations of somatosensory cortex. Neurology, 1988, 38: 1705–1714.

Towle, V.L., Bolanos, J., Suarez, D., Tan, K., Grszeszcuk, R., Levin, D.N., Cakmur, R., Frank, S.A. and Spire, J.-P. The spatial location of EEG electrodes: locating the best-fitting sphere relative to cortical anatomy. Electoenceph. clin. Neurophysiol., 1993, 86: 1–6.

Van Oosterom, A. History and evaluation of methods for solving the inverse problem. J. Clin. Neurophysiol., 1991, 8: 371–380.

Woolsey, C.N., Erickson, T. and Gilson, W.E. Localization in somatic sensory and motor areas of human cerebral cortex as determined by direct recording of evoked potentials and electrical stimulation. J. Neurosurg., 1979, 51: 476–506.